International Journal of Nanomedicine

Dovepress
open access to scientific and medical research

Open Access Full Text Article

ORIGINAL RESEARCH

Comparison of normal versus imiquimod-induced psoriatic skin in mice for penetration of drugs and nanoparticles

This article was published in the following Dove Press journal:
International Journal of Nanomedicine

Lin Sun[1,2]
Zeyu Liu[1]
Zibei Lin[1]
Dongmei Cun[3]
Henry HY Tong[4]
Ru Yan[1]
Ruibing Wang[1]
Ying Zheng[1]

[1]State Key Laboratory of Quality Research in Chinese Medicine, Institute of Chinese Medical Sciences, University of Macau, Macao Special Administrative Region, People's Republic of China; [2]Department of Pharmaceutical Sciences, Zhuhai Campus of Zunyi Medical University, Zhuhai, Guangdong, 519041, People's Republic of China; [3]Department of Pharmaceutical Sciences, Shenyang Pharmaceutical University, Shenyang, Liaoning, 110016, People's Republic of China; [4]School of Health Sciences, Macao Polytechnic Institute, Macao Special Administrative Region, People's Republic of China

Background: As an immune-mediated skin disease, psoriasis encounters therapeutic challenges on topical drug development due to the unclear mechanism, and complicated morphological and physiological changes in the skin.

Methods: In this study, imiquimod-induced psoriatic mouse skin (IMQ-psoriatic skin) was chosen as the in vitro pathological model to explore the penetration behaviors of drugs and nanoparticles (NPs).

Results: Compared with normal skin, significantly higher penetration and skin accumulation were observed in IMQ-psoriatic skin for all the three model drugs. When poorly water-soluble curcumin was formulated as NPs that were subsequently loaded in gel, the drug's penetration and accumulation in both normal and IMQ-psoriatic skins were significantly improved, in comparison with that of the curcumin suspension. Interestingly, the NPs' size effect, in terms of their penetration and accumulation behaviors, was more pronounced for IMQ-psoriatic skin. Furthermore, by taking three sized FluoSpheres® as model NPs, confocal laser scanning microscopy demonstrated that the penetration pathways of NPs no longer followed the hair follicles channels, instead they were more widely distributed in the IMQ-psoriatic skin.

Conclusion: In conclusion, the alternation of the IMQ-psoriatic skin structure will lead to the enhanced penetration of drug and NPs, and should be considered in topical drug formulation and further clinical practice for psoriasis therapy.

Keywords: imiquimod-induced psoriatic skin, pathological model, topical delivery, penetration, nanoparticles

Introduction

Psoriasis is a common and relapsing skin disease, which is characterized by desquamation, erythema, epidermis thickening, and plaque-like skin lesions.[1] Multiple genetic, immunologic, and environmental factors[2] can induce the emergence of psoriasis, including trauma, drugs, infection, humidity, and stress.[3] It is generally accepted that the initial stimulation of dendritic cell in the skin results in a complicated crosstalk between keratinocytes and immune system, resulting in the epidermal hyperplasia, parakeratosis, and leukocytes infiltration in the skin.[4] Stimulation of dendritic cells (DCs) leads to antigen-presentation, which triggers the release of immune mediators. Psoriatic inflammation results from pro-inflammatory cytokines, such as interleukin (IL) 1β, and tumor necrosis factor released by DCs, which is critically mediated by chemokine receptor 6.[5] Activation of IL 23 induces the production of IL 17A and IL 22 and also gives rise to psoriatic lesion.[6] As for the relapse and chronicity of psoriasis, IL-17-producing T cells play an important role.[7] For therapy, 90% of the patients are

Correspondence: Ying Zheng
State Key Laboratory of Quality Research in Chinese Medicine, Institute of Chinese Medical Sciences, University of Macau, 6/F, Rm 6010, N22, Macao Special Administrative Region, People's Republic of China
Tel +86 853 8822 4687
Fax +86 853 2884 1358
Email yzheng@umac.mo

submit your manuscript | www.dovepress.com
Dovepress
http://dx.doi.org/10.2147/IJN.S170832

treated using topical formulations, due to their affordable, safe, and convenient administration. Besides classical anti-psoriatic drugs including topical corticosteroids, vitamin D analogs, and tar-based preparations,[8] and active agents in traditional Chinese medicines, nanotechnology is also utilized to improve the drug penetration and bioavailability[9] by enhancing drugs' affinity to skin barriers[10] or by improving the physicochemical properties of drug for topical delivery.

As an immune-related skin disease, psoriasis can promote activated T cells to induce the expression of inflammatory factors and accumulation of inflammatory cells in dermis, following the weakening stratum corneum (SC), hyperkeratosis, and parakeratosis in the skin.[11] During the development and evaluation process of anti-psoriatic topical formulations, these changes on the morphological and pathological functions of the diseased skin cannot be truly reflected by the in vitro penetration model using the healthy skin. However, there are few studies to investigate and compare the penetration behaviors of drugs and nanoparticles (NPs) formulation in psoriatic skin, the understanding of which may ultimately affect the design and development of anti-psoriatic topical formulations. In 2015, imiquimod (IMQ)-induced psoriatic skin (IMQ-psoriatic skin) was utilized to estimate the in vitro penetration behavior of drugs by Lin et al[12] for the first time, whose research demonstrated much higher penetration of drug through IMQ-psoriatic skin, than through normal skin. The study also showed that the lipophilicity of a drug dictated the permeation behaviors of the drug in IMQ-psoriatic lesions. However, their results were obtained under different donor and acceptor systems, which intrinsically make the active pharmaceutical ingredients (APIs) present a different penetration ability. Moreover, the penetration behavior of NP systems, which represents an important delivery strategy for topical delivery today, has not been addressed in their work.

IMQ is an innate TLR7/8 immune activator which can induce and exacerbate psoriasis on mice and human skin.[13] Since 2009, the IMQ-induced psoriasis-like mouse model, the process of which is rapid and convenient, has been increasingly utilized in in vivo evaluations of psoriasis and its therapy in many recent studies.[14] Although this model only presents a part of the characteristics in psoriasis, it is still critically dependent on the IL-23/IL-17 axis, resembling the expression of IL-17, IL-22, and IL-23 in IMQ-psoriatic skin, also the symptoms of desquamation, erythema, and thickening.

With the aim to investigate penetration behavior and pathway alternations of drugs and nanoparticles under psoriasis conditions, IMQ-psoriatic skin and normal skin were used as the two in vitro penetration barrier models. Three widely used drugs in transdermal drug delivery systems with different partition coefficients, namely, indomethacin (IM), lidocaine (LD), and 5-fluorouracil (5-FU), which are shown in Figure 1,[15,16] have been chosen as the model drugs. Identical donor and acceptor systems, which are isopropyl myristate (IPM) and phosphate buffer saline (PBS, pH =7.4) solution, were utilized to maintain the homogeneous background for comparison. In addition, to

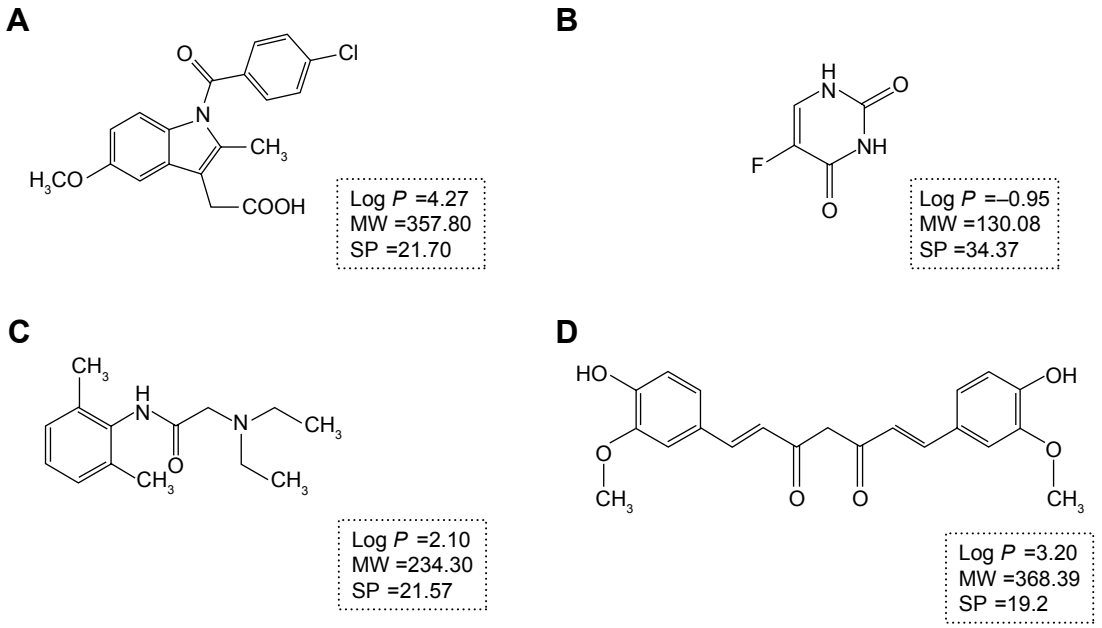

Figure 1 The chemical structures and properties of indomethacin (**A**), 5-fluorouracil (**B**), lidocaine (**C**), and curcumin (**D**). The SP value in **A**, **B**, and **C** was from Meng et al,[16] while the SP value in **D** was from Zhao et al.[15]
Abbreviations: MW, molecular weight (g/mol); SP, solubility parameter ($MPa^{1/2}$).

evaluate the penetration behaviors of polymeric NPs, two differently sized poly (lactic-*co*-glycolic acid) (PLGA) NPs have been fabricated and evaluated where the anti-psoriatic agent curcumin (Cur) is selected as the model drug in the NPs formulation. Mechanistic investigation by confocal laser scanning microscopy (CLSM) was conducted to observe the penetration pathway of three different sized FluoSpheres®, non-degradable, commercially available polystyrene carboxylated NPs, which have been widely used in fluorescent tracing study[17] and in topical delivery of NPs.[18]

Materials and methods

Materials

IMQ topical cream was purchased from Aldara (5% imiquimod; Health Care Limited, Loughborough, UK). IM (I106885, 99%), 5-FU (F100149, 99%), and IPM (I109490, 98%) were obtained from Aladdin Industries Corporation (Shanghai, People's Republic of China). LD (L0156, 99%) was supplied by TCI Development Co., Ltd (Shanghai, People's Republic of China). Curcumin was obtained from Yung Zip Chemical Industries Ltd. (Taichung, Taiwan, People's Republic of China), while PLGA (50:50 LA: GA [w:w], 5,000 Da) was purchased from Wako Pure Chemical Industries Ltd. (Tokyo, Japan). Polyvinylpyrrolidone (PVP) was obtained from Wing Hing Chemical Company Ltd. (BP grade, Hong Kong, People's Republic of China). Carbopol 974 was supplied by Chineway (Shanghai, People's Republic of China). FluoSpheres® with the catalog No of F8789 (40 nm), F8801 (100 nm), and F8813 (500 nm), were purchased from Thermo Fisher (Eugene, OR, USA). Paraformaldehyde (4%) was obtained from Jingxin Biological Technology (Guangzhou, People's Republic of China). Methanol and acetonitrile were obtained from Merck (Darmstadt, Germany). Milli-Q water was obtained from a Millipore Direct-Q ultra-pure water system (Millipore, Bedford, USA). Absolute ethanol was purchased from Tianjin Kaitong Chemical Reagent Co. Ltd. (Tianjin, People's Republic of China).

Animals

Female C57/BL6 mice (7–9 weeks old) were supplied and housed under specific pathogen free conditions by the Experimental Animal Center of Faculty of Health Sciences, University of Macau (Macao Special Administrative Region of the People's Republic of China). The University of Macau Animal Ethics Committee approved all the animal protocols used (Protocol No: UMAEC-022–2015). All experiments were carried out in accordance with the NIH Guidelines for the Care and Use of Laboratory Animals.

Establishment and evaluations of imiquimod-induced psoriasis-like mouse model

IMQ is a TLR7/8 ligand and a potent immune activator. The topical application of IMQ can induce and exacerbate psoriasis.[19] van der Fits et al provided a modifying procedure to develop the psoriasis-like model.[13] Female C57BL/6 mice were treated with IMQ (62.5 mg of commercially available IMQ cream [5%], corresponding to a daily dose of 3.125 mg of the active compound) on the shaved back every 24 hours for 6 days. On day 7, the mice were scarified by the inhalation of CO_2 (Smartbox Auto CO_2 system, Euthanex, PA, USA).

After establishment of the model, hematoxylin and eosin (H&E) staining as well as immunohistochemistry (IHC) studies were performed. The treated dorsal skin was obtained at the end of the experiment, and then fixed in 4% paraformaldehyde. After they had been embedded in paraffin, 4 μm microtome sections of skin samples were obtained. Then samples were divided into two parts; one of them was used to do H&E staining. Samples were deparaffinized, rehydrated, and stained with H&E. An IHC study for IL-17, IL-22, and IL-23 was performed using another part of samples. Briefly, paraffin-embedded samples were washed in xylene and hydrated in different concentrations of alcohol, and then incubated with primary antibody against IL-17 (ab79056, Abcam), IL-22 (ab18499), IL-23 (ab115759), and isotype (ab27472) separately overnight at 4°C. Horseradish peroxidase-conjugated secondary antibody was applied to bind with the primary antibody for detection. The sections were stained with 3,3′-diaminobenzidine chromogen and counterstained with hematoxylin. Brown staining was considered as a positive identification for the primary antibodies. A microscope equipped with a computer-controlled digital camera (BDS 200, Aote, People's Republic of China) was used to visualize the sections.

Preparation of IMQ-psoriatic and normal skins

The skin preparation was performed according to the procedure described in a previous report with a few modifications.[20] Female C57/BL6 mice were anesthetized using chloral hydrate (4%, 0.1 mL/10 g, i.p.) and shaved carefully using a clipper and an electrical shaver. Full-thickness skin was excised after the mice had been sacrificed. The integrity of the skin was checked carefully with microscopy, and any skin that was not uniform was rejected. After removing the subdermal tissue, the skin was washed with PBS, and then stored

at −80°C until required. Before use, the skin was thawed to room temperature. The induction process of IMQ-psoriatic skin on mice backs is described in the previous section. The procedure from scarification was performed in the same manner as the preparation method of the normal skin.

Preparation of Cur-NPs

Cur-NPs of 50 and 150 nm were fabricated and characterized according to our previously published data.[21] Briefly, Cur and PLGA were dissolved (1:1, w/w, 5 mg/mL) in dimethylformamide to form the organic phase, while PVP (0.8 mg/mL) was chosen as the stabilizer in the aqueous phase. The larger-sized NPs were fabricated by injecting the organic phase into the aqueous phase (1:5, v/v) with stirring at 900 rpm. A home-made multi-inlet vortex mixer, consisting of four inlet streams, was used to fabricate smaller-sized Cur-NPs. One of the inlet streams was an organic phase with the same composition described above, and one inlet stream consisted of an aqueous solution of PVP at a concentration of 0.4 mg/mL. The other two streams were both Milli-Q water. The pump (Harvard Apparatus, PHD 2000; Cambridge, MA, USA) speed was set at 10:90 mL/min (organic phase and one of the tunnels of water:aqueous phase and one of the tunnels of water). The size of the two NPs was 48.89±0.19 nm (PDI =0.11±0.01) and 152.00±1.39 nm (PDI =0.10±0.01), respectively, with the encapsulation efficiency of 96.45% ± 1.53% and 92.48% ± 0.14%, respectively. About 90% of Cur could be released from the two NPs during 72 hours exposure in PBS (pH =7.4).

Preparation of drug loaded hydrogels

Topical formulations should have adequate viscosity to be applied onto the skin. Carbopol was chosen as the matrix of the Cur suspension (diluted water as solvent) and Cur-NPs. For Cur-NPs, Carbopol of 1% (w/v) was slowly added into the suspension with slow, constant stirring in darkness for 24 hours. After swelling adequately, the gel was neutralized to pH 6 by drop-wise addition of triethanolamine. For drug suspension-loaded gel, Cur was added into the blank Carbopol gel, which was prepared by adding triethanolamine and propylene glycol. The Cur concentration was 0.025% (w/w) in the gel.

In vitro skin permeation studies

For the drug in IPM solution, normal and IMQ-psoriatic mouse skins were mounted on side-by-side diffusion cells (PermeGear H3, USA) with the SC of skin facing the donor solution. For the drug in gel, mouse skin was mounted on a Franz cell (PermeGear V6-CA, USA) with the SC facing up. The graphical presentation of the penetration experiments is shown in Figure 2. The capacity of donor and receiver parts of the Franz cell was 2.0 and 8.0 mL, respectively, while the volume of the side-by-side cell was 3.0 mL for both. The effective diffusion area was 1 cm^2. The two cells were clamped securely using a clip and connected to a water bath at 32°C, which is the temperature of human skin. Different drug formulations were added in the donor cells, while the corresponding receptor solution was added to the acceptor cells with continuous stirring to maintain the sink conditions. A sample of 1 mL (for Franz cell) or 2 mL (for side-by-side cell) was withdrawn from acceptor cells and supplemented with fresh receptor solution at predetermined intervals. The experiments were performed for 8 hours for IPM solution system, or 24 hours for cream and gel systems. Other penetration conditions are summarized in Table 1. The skin was washed three times using receptor solution

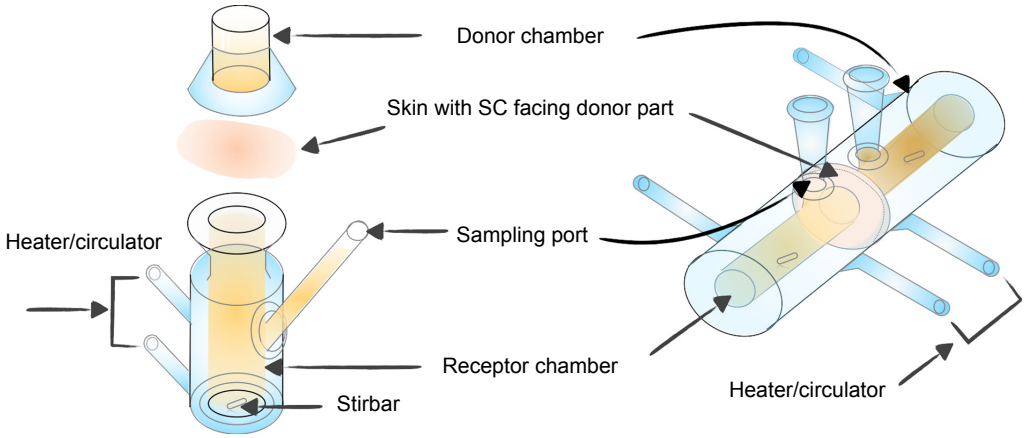

Figure 2 The Franz cell (left part) and the side-by-side diffusion cell (right part) used for in vitro skin permeation studies.
Abbreviation: SC, stratum corneum.

Table 1 Conditions for penetration studies of drug solutions and NPs

Order number	APIs	Drug form	Donor cell	Receiver cell	Duration
1	LD	Free drug	Supersaturation in IPM, 3 mL	PBS (pH =7.4), 3 mL	8 h
2	IM	Free drug	Supersaturation in IPM, 3 mL	PBS (pH =7.4), 3 mL	8 h
3	5-FU	Free drug	Supersaturation in IPM, 3 mL	PBS (pH =7.4), 3 mL	8 h
4	Cur	Free drug	Suspended in gel, 0.25 mg/mL, 2 g	20% ethanol–water, 8 mL	24 h
5	Cur	50 nm NPs	NPs in gel, 0.25 mg/mL, 2 g	20% ethanol–water, 8 mL	24 h
6	Cur	150 nm NPs	NPs in gel, 0.25 mg/mL, 2 g	20% ethanol–water, 8 mL	24 h

Note: The experiments were performed at 32°C.
Abbreviations: 5-FU, 5-fluorouracil; APIs, active pharmaceutical ingredients; Cur, curcumin; IM, indomethacin; IPM, isopropyl myristate; LD, lidocaine; NPs, nanoparticles.

and wiped. After cutting into pieces, the skin was subjected to ultrasonic extraction for 30 minutes in 80% aqueous acetonitrile. After centrifugation (12,500× *g*, 10 minutes), the sample was measured with HPLC or LC-MS/MS. Experiments were performed in triplicates, with each skin sample obtained from different mouse.

The drug deposition in the skin and the cumulative amount of permeated drug were calculated, which was obtained from the measured concentration and volume of the receiver phase. The cumulative amount (Q) of APIs permeated through the skin was plotted as a function of time. The slope of the linear portion of the plot was calculated as the steady-state flux (J_{ss}). The enhancing ratio of penetration flux (ER_J), representing the effect of IMQ-psoriatic skin on drug penetration process, was calculated using the equation $ER_J = J_{ss}$ (IMQ-psoriatic skin)/J_{ss} (normal skin), while the enhancing ratio of skin accumulation (ER_S), representing the effect of IMQ-psoriatic skin on drug accumulation in the skin, was calculated using the equation ER_S = drug accumulation in IMQ-psoriatic skin/drug accumulation in normal skin.

CLSM observation

Three different FluoSpheres® with the particle size of 40 nm (F8793), 100 nm (F8801), and 500 nm (F8813) were chosen as the model nanoparticles, where the first two presented red (580/605) and the last one presented green (505/5153) fluorescence. FluoSphere® was diluted to 1% solid with Milli-Q water and applied on the donor side of Franz cells for both normal and IMQ-psoriatic skin penetration. Milli-Q water was filled in the acceptor side, with the circulation maintained at 32°C for 24 hours. The skin was harvested and washed with water at the predetermined time. Freezing microtome section was made using a Leica CM1905 cryostat (Leica Biosystems, Buffalo Grove, IL, USA) with the thickness of 20 µm. The slides were examined using CLSM (Leica TCS SP8, Solms, Germany). For acquiring images, the excitation wavelength was 552 nm and emission wavelengths were between 590 and 656 nm for 40-nm- and 100-nm-sized FluoSphere® detection, while the excitation wavelength was 488 nm and emission wavelengths were between 495 and 545 nm for 500-nm-sized FluoSphere® detection.

Analytical methods

The penetration of Cur and Cur-NPs was measured using an ABI 4000 Q-Trap™ hybrid triple quadrupole linear ion trap mass spectrometer (Applied Biosystems, Foster City, CA, USA) with a Turbo V ionization source operated in the negative ion mode and coupled to an Agilent 1200 HPLC system (Agilent Technologies, CA, USA). The separation was performed using a C18 reversed-phase column (Zorbax extend C18, 100×2.1 mm i.d., 3.5 µm, Agilent, USA). The flow rate was 0.4 mL/min, and the injection volume was 10 µL. The mobile phase consisted of 0.1% aqueous formic acid (A) and acetonitrile (B) and eluted in a gradient mode, which was adopted as follows: 0–2 minutes, 10% B; 2–4 minutes, 10%–90% B; 4–9 minutes, 90%; 9–10 minutes, 90%–10% B; 10–12 minutes, 10% B. The quantification was performed using a multiple-reaction monitoring mode with the transitions of m/z 367.1→134.0 for Cur and 268.0→225.0 for emodin (IS). The main working parameters were set as follows: ion-spray voltage, –5,500 V; ion source temperature, 500°C; gas 1, 40 psi; gas 2, 40 psi; and curtain gas, 20 psi. The concentrations of the analytes were determined using the software Analyst 1.5 software (Applied Biosystems, CA, USA).

The penetration samples of other drugs were measured using an Agilent 1200 Series HPLC system (Agilent, USA) equipped with a DAD detector. Analyses were performed using an Agilent Zorbax SB-C18 column (250×4.6 mm, 5 µm, Agilent) at room temperature. The injection volume for all samples was 10 µL. The flow rate was 1 mL/min. The mobile phase was acetonitrile: phosphate buffer solution (0.5 mol/L Na_2HPO_4, 32.5 mL and 1 mol/L NaH_2PO_4, 1.3 mL, diluted to 1,000 mL with water) (65:35, v/v) for LD, acetonitrile: 0.1 mol/L ethylic acid solution (6:4, v/v) for IM, 5% aqueous methanol solution for 5-FU. The monitoring

wavelength was set at 254, 228, and 265 nm for LD, IM, and 5-FU, respectively.

Statistical analysis

Results were expressed as mean ± SE. The statistical significance of the differences between the normal and IMQ-psoriatic skins was tested with paired-sample *t*-test analysis using the SPSS software, where $P<0.05$ was considered statistically significant.

Results and discussion

Model establishment and validation

IMQ-induced psoriasis-like mouse model is a widely used pathological model for various in vivo evaluations. Besides the apparent simulation of psoriatic symptoms, the IL-23/IL-17 axis also takes an important role in the induction progress of this disease. As shown in Figure 3A1, the symptoms of psoriasis, including erythema, desquamations, and thickening, were recorded on the dorsal skin of the mice after 7-day treatment by IMQ. To further validate this psoriasis-like model, H&E staining and IHC studies were performed. As shown in Figure 3B, remarkable hyperkeratosis and parakeratosis (nuclei in the SC) were observed in the H&E stained image. IHC results from the IMQ-treated dorsal skin further showed increased IL-17, IL-22, and IL-23-positive cells in the skin (Figure 3C–E), indicating the characteristic expression of inflammatory factors, which participated in the progression of psoriasis. Taken together, the results of H&E staining and IHC of the normal and IMQ-psoriatic skins demonstrated the formation of psoriasis-like skin, which partially mimicked the real psoriatic skin morphologically and pathologically.

In vitro penetration behavior of model drugs in IPM solution

The penetration results of three model drugs in IPM solution are summarized in Table 2. Higher Q_8, flux, and skin accumulation amount were obtained from the IMQ-psoriatic skin for all the three APIs. Among them, the highest ER_J and ER_S were from 5-FU, indicating the IMQ-psoriatic skin presented the strongest effect on the penetration flux and skin accumulation of 5-FU that is the most hydrophilic drug (log P= −0.95) among these three model APIs. SC is the major barrier for hydrophilic agents, while the rate-limiting step for lipophilic agents is the distribution route from SC to dermis.[22] The disrupted SC in IMQ-psoriatic skin dramatically reduced the first penetration barrier for hydrophilic 5-FU, endowing outstanding high value of ER_s (5.78). It is speculated that after passing through the SC, the effect of loose barrier of the IMQ-psoriatic skin on the penetration behavior of 5-FU was reduced, whereas the distribution route from epidermis to dermis dominated and restricted the penetration of the drug, resulting in the increased drug accumulation in the skin.

The pathological skin condition also promoted the skin penetration of IM, where ER_J and ER_s were 2.06 and 3.56,

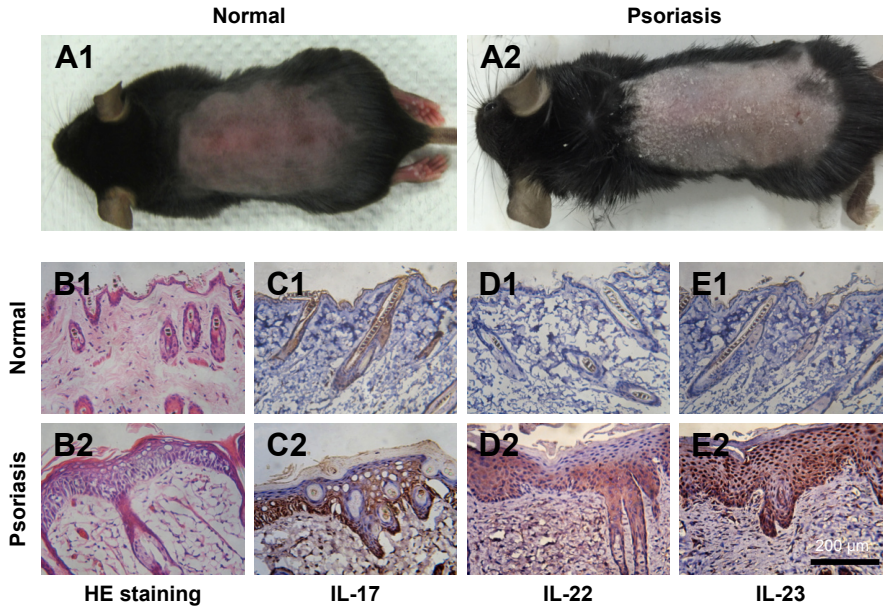

Figure 3 Topical application of imiquimod-induced psoriatic like change on the dorsal skin of mice.
Notes: At day 7, photographs were taken from the mice (**A1**, **A2**) and H&E staining (**B1**, **B2**, ×250 magnification) was performed to observe the differences of between the normal skin (**A1** and **B1**) and IMQ-psoriatic skin (**A2** and **B2**). Immunohistochemistry of IL-17 (**C**), IL-22 (**D**), and IL-23 (**E**) were performed on both normal (**C1**–**E1**) and imiquimod-psoriatic skin (**C2**–**E2**).

Table 2 Permeation parameters of IM, LD, and 5-FU solution through mouse skin at 32°C

APIs	Skin	Q_8 (μg·cm^{-2})	J_{ss} (μg·h^{-1}·cm^{-2})	Drug in skin (μg·cm^{-2})	ER_J	ER_S
IM	Normal	195.43 ± 42.61	34.66 ± 7.04	170.00 ± 29.47	2.06	3.56
	IMQ-psoriatic	395.35 ± 88.70[a]	71.43 ± 18.24[a]	605.64 ± 157.62[a]		
LD	Normal	2,293.82 ± 439.59	322.94 ± 79.90	114.98 ± 37.02	1.55	1.80
	IMQ-psoriatic	3,689.45 ± 381.08[a]	500.64 ± 80.26	206.70 ± 74.06		
5-FU	Normal	173.78 ± 52.87	22.98 ± 4.90	140.26 ± 9.48	2.08	5.78
	IMQ-psoriatic	361.16 ± 38.84[a]	41.60 ± 14.18[a]	810.86 ± 210.42[a]		

Notes: Data are given as mean ± SE (n=3). Q_8, penetration amount through skin accumulated during 8 h; J_{ss}, steady-state flux; $ER_J = J_{ss}$ (IMQ-psoriatic skin)/J_{ss} (normal skin), ER_S = drug accumulation in skin (IMQ-psoriatic skin)/drug accumulation in skin (normal skin). [a]Significantly different from that of corresponding normal skin ($^aP<0.05$).
Abbreviations: 5-FU, 5-fluorouracil; IM, indomethacin; IMQ, imiquimod; LD, lidocaine.

respectively. All the penetration behaviors in IMQ-psoriatic skin of both 5-FU and IM seemed significantly different from their behaviors in the normal skin ($P<0.05$). Conversely, although LD showed good penetration ability through the normal skin, the IMQ-psoriatic barrier did not significantly affect its penetration behavior. Both IM and LD are typical lipophilic transdermal agents, with the log *P*-values of 4.27[23] and 2.10,[24] respectively. Although the log *P*-value of LD was lower, the solubility of LD in IPM and water (211.25 and 6.81 mg/mL,[25] respectively) at 32°C is much higher than those of IM (2.10 and 0.07 mg/mL,[26] respectively), indicating an excellent balancing between the hydrophilic and lipophilic properties, which may facilitate the transdermal drug delivery. In addition, for the solubility parameter (SP) of these three APIs, the lowest value was from LD (21.57 MPa$^{1/2}$), which is closest to the SP of skin (20.5 Mpa$^{1/2}$),[27] indicating a high compatibility with the lipid in SC and a potent permeability through the skin. Actually, as the value of SP increased, the ER_J and ER_S values also increased (21.70 and 34.37 MPa$^{1/2}$ for IM and 5-FU, respectively[16]), which could be speculated that the psoriasis disturbed the arrangement of lipid in the skin, providing the low compatibility and permeability drug more chance and enhancement to penetrate through the IMQ-psoriatic skin.

The application of IMQ-psoriatic skin was first reported by Lin et al[12] for in vitro evaluation. Several anti-psoriatic drugs were utilized in different donor and acceptor systems to compare drug penetration between the normal and IMQ-psoriatic skins. However, the type of donor solutions, especially with or without organic solvent, would greatly influence the reliability of the results. To overcome this problem, IPM and PBS solutions were selected in this work as the identical donor and acceptor systems, respectively. IPM is a classical matrix in penetration evaluation of a transdermal drug delivery system, which is an analog of ceramide, a main component of the lipid in SC.[28] In this study, IPM was used to mimic the skin conditions, whereas the PBS buffer (pH =7.4) was used to mimic the systemic conditions. We believe that under the same condition, more reliable comparison could be drawn from the results.

In vitro penetration behavior of Cur-NPs in gel

Carbopol gel is a widely used semisolid matrix for topical formulations. Appropriate rheological properties enable the formulation to remain on the skin thereby enhancing the therapeutic efficacy of delivered drugs. In consideration of the common clinical practice, the influence of IMQ-psoriatic skin on drugs in gel systems was also investigated in this work. As a potent anti-psoriatic agent from Chinese medicine, Cur was chosen as the model drug.

First, the penetration properties of Cur between Cur suspension and Cur-NPs were compared. Results showed that both the cumulative amount of permeated drug and drug accumulation in the skin were dramatically improved by fabricating Cur as Cur-NPs in gel (Table 3), which might be attributed to the better stability and solubility of Cur in NPs gel formulations.[29] Second, penetration behaviors of Cur suspension and Cur-NPs in gel were compared on both the normal and IMQ-psoriatic skins. As shown in Table 3, in all the three formulations, including Cur suspension in gel, 50-nm-sized Cur-NPs in gel, and 150-nm-sized Cur-NPs in gel, the drug accumulation in the IMQ-psoriatic skin was much higher than that in the normal skin (the ER_S value was 1.70, 1.13, and 1.44, respectively). Similarly, the cumulative amount of permeated drug Q_{24} in the IMQ-psoriatic skin was much higher than that in the normal skin in the suspension (238.84±27.65 and 461.19±39.46 ng·cm^{-2} in normal and IMQ-psoriatic skins, respectively) and 50 nm NPs groups (1,071.02±32.67 and 1,308.70±72.25 ng·cm^{-2} in normal and psoriatic skins, respectively); however, the Q_{24} value in the normal and diseased skins was similar for the group of 150 nm NPs (1,119.10±112.88 and 897.36±88.36 ng·cm^{-2} in normal and IMQ-psoriatic skins, respectively). Third, the size effects on drug penetration amount and drug accumulation in the skin were more prominent in the IMQ-psoriatic skin.

Table 3 Permeation parameters of Cur from the gel with different formulations through excised normal and IMQ-psoriatic skins at 32°C

Drug form	Skin	Q_{24} (ng·cm^{-2})	J_{ss} (ng·h^{-1}·cm^{-2})	Drug in skin (ng·cm^{-2})	ER_J	ER_S
Cur suspension in gel	Normal	238.84 ± 27.65	6.85 ± 0.61	766.67 ± 173.98	1.32	1.70
	IMQ-psoriatic	461.19 ± 39.46[a,b]	9.06 ± 0.51[a]	1,311.00 ± 254.15[a,b]		
50 nm Cur-NPs in gel	Normal	1,071.02 ± 32.67	29.13 ± 1.90	2,560.00 ± 263.50	1.55	1.13
	IMQ-psoriatic	1,308.70 ± 72.25[a,b]	45.24 ± 2.13[a]	2,903.33 ± 530.42[b]		
150 nm Cur-NPs in gel	Normal	1,119.10 ± 112.88	28.96 ± 0.20	3,063.33 ± 328.45[c]	0.80	1.44
	IMQ-psoriatic	897.36 ± 88.36[b,c]	22.97 ± 0.95[a,c]	4,410.00 ± 665.23[a–c]		

Notes: Data are given as mean ± SE (n=3). Q_{24}, penetration amount through skin accumulated during 24 h; J_{ss}, steady-state flux; $ER_J = J_{ss}$ (IMQ-psoriatic skin)/J_{ss} (normal skin), ER_S = drug accumulation in skin (IMQ-psoriatic skin)/drug accumulation in skin (normal skin). [a]Significantly different from that of corresponding normal skin group, $^aP<0.05$; [b]the penetration parameters of Cur from the gel with different formulations through excised IMQ-psoriatic skin were from our published data; [c]significantly different between the two sized Cur-NPs in gel groups.

Abbreviations: Cur, curcumin; IMQ, imiquimod; NPs, nanoparticles.

The small-sized NPs in gel showed a significantly higher penetration through the IMQ-psoriatic skin than that through the normal skin, while the higher skin accumulation was obtained from the 150-nm-sized NPs in gel. For NPs systems, the improved penetration of 50-nm-sized Cur-NPs and improved skin accumulation of 150-nm-sized Cur-NPs may be attributed to the loosening of SC, which allowed more NPs to immerse into the epidermis, and subsequently to penetrate through the skin with higher permeability.

CLSM observation of FluoSphere®

After incubation with different sized FluoSpheres® for 24 hours, the normal or psoriatic skins were prepared to vertical sections with 20 μm thickness, and visualized using CLSM (Figure 4). Skin penetration and distribution of 40-, 100-, and 500-nm-sized NPs are presented in red color in Figure 4A (200×) and 4B (1,260×), respectively. Each figure consists of panels showing the fluorescent signals (by the fluorescein of FluoSphere®), bright field signals,

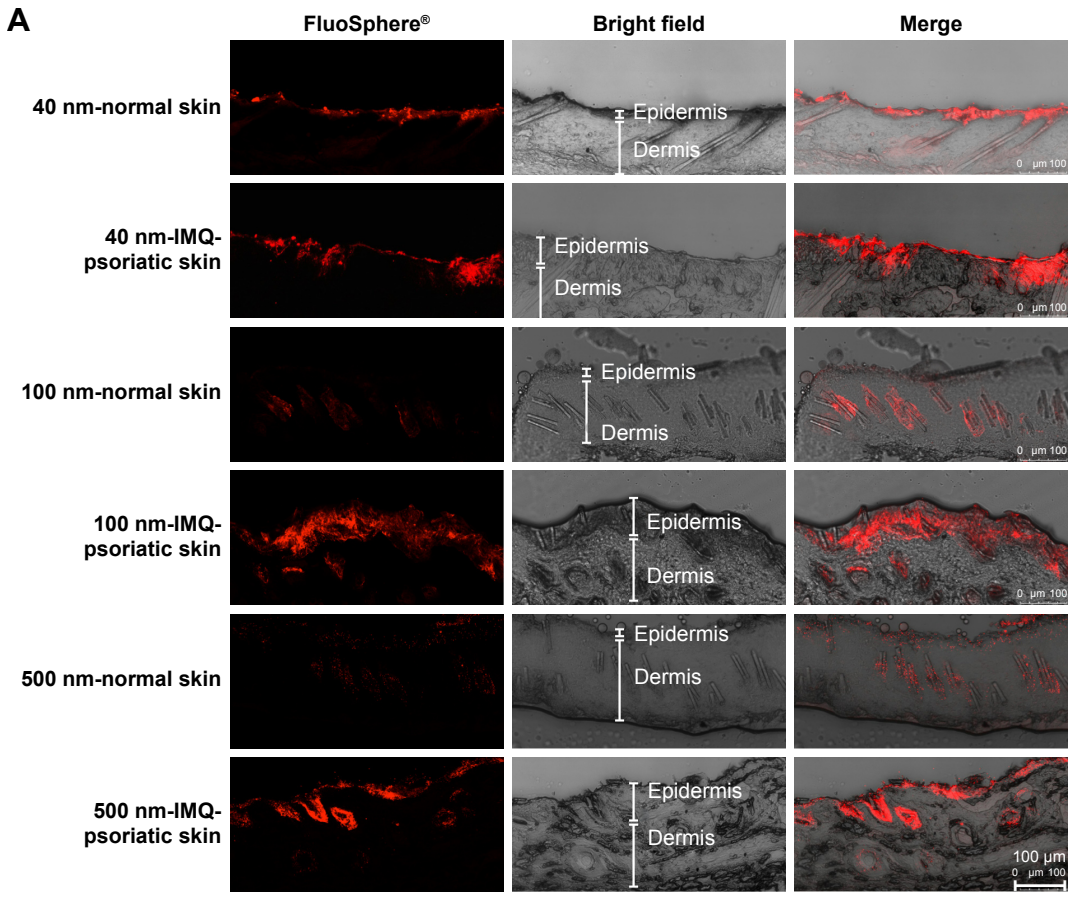

Figure 4 (*Continued*)

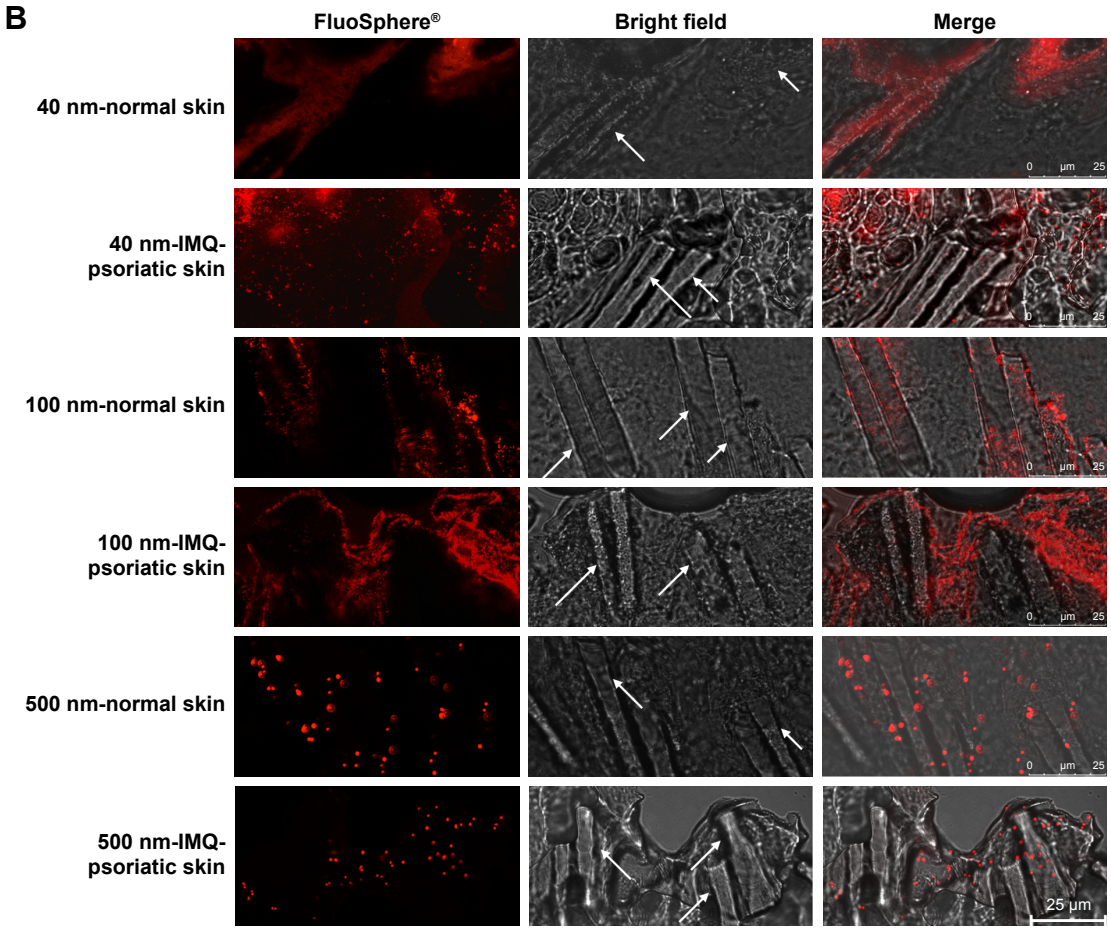

Figure 4 CLSM visualization of vertical sections from normal and imiquimod-induced psoriatic skins, which were treated with 40-, 100-, and 500-nm-sized FluoSpheres® for 24 hours at 32°C.

Notes: Two views were given to present the wide structure of skin penetration (**A**, 200×), as well as the enlarged field of the distribution around hair follicles (**B**, 1,260×). For picture **A**, bar =100 μm, while for picture **B**, bar =25 μm. The emission wavelength was between 590 and 656 nm for 40 and 100-nm-sized FluoSphere® when the excitation wavelength was set as 552 nm, while the emission wavelength was between 495 and 545 nm for 500-nm-sized FluoSphere® when the excitation wavelength was set as 488 nm. The white arrows indicate the hair follicles.

Abbreviations: CLSM, confocal laser scanning microscopy; IMQ, imiquimod.

and a superimposition of both signals. Two views of the normal or IMQ-psoriatic skin were given to present the wide structure of skin penetration, as well as the enlarged field of the distribution around hair follicles. The wide structure of bright field images showed epidermis thickening of IMQ-psoriatic skin.

The vertical sections of the IMQ-psoriatic skin samples exposed to FluoSphere® showed that the fluorescent signal was increased in comparison with that in the normal skin. For all the three sized NPs, the dye of FluoSphere® was found to be deposited homogeneously into the epidermis of the IMQ-psoriatic skin. In contrast, the dye was found only around the hair follicle in the normal skin. In addition, for 500-nm-sized FluoSphere®, the fluorescence intensity was much lower and the distribution was more dispersive than the two smaller-sized NPs in both normal and IMQ-psoriatic skins.

As shown in Figure 4, the fluorescence of 40- and 100-nm NPs was similar in the normal skin, which was much higher than that of 500-nm-sized NPs, indicating that the reduction of particle size facilitates skin accumulation. However, there was a little difference between the 40- and 100-nm-sized NPs, in which the 100-nm-sized NPs demonstrated slightly higher accumulation in the IMQ-psoriatic skin. It was speculated that the 100-nm-sized NPs had more chance to accumulate in the follicles and upper layer of the epidermis due to the larger size, whereas the 40-nm-NPs might have more opportunity to penetrate through the entire skin, even into the systemic circulation.

As shown in rows 1, 3, and 5 of Figure 4B, the major pathway of NPs through the normal skin is hair follicle, which has been demonstrated in several studies for years.[18,30] The distribution and penetration pathway of NPs through the IMQ-psoriatic skin seems different from the widely established hair follicle pathway, in which epidermis in the pathological model permitted wider and more extensive penetration of NPs (Figure 4A, rows 2, 4, and 6). In addition to

hair follicles, the NPs, especially the small-sized ones, could penetrate through the pathological epidermis to dermis layer, resulting in the higher accumulation and penetration in the pathological model (Table 3).

Conclusion

Compared with normal mice skin, enhanced drug permeation and skin accumulation were observed for drug solution, suspension, and drug NPs in gel using in vitro IMQ-induced psoriatic skin model, which seems related to high hydrophilicity or low intrinsic penetration ability of drugs. The IMQ-psoriatic skin improves the penetration of NPs by altering the pathway because the changed skin structure in IMQ-psoriatic condition gives more chance for NPs to penetrate beside the hair follicles. Therefore, alternation of IMQ-psoriatic skin structure and transdermal capacity of relevant drugs or nanoparticles should be taken into consideration for future development of anti-psoriatic agents and clinical therapeutic practice.

Acknowledgments

This work was supported by a research grant from the University of Macau (number: MYRG2014-00040-ICMS-QRCM) and Macao Science and Technology Development Fund (number: 0013/2018/A1).

Disclosure

The authors report no conflicts of interest in this work.

References

1. Lowes MA, Bowcock AM, Krueger JG. Pathogenesis and therapy of psoriasis. *Nature*. 2007;445(7130):866–873.
2. Slominski AT, Zmijewski MA, Skobowiat C, Zbytek B, Slominski RM, Steketee JD. Sensing the environment: regulation of local and global homeostasis by the skin's neuroendocrine system. *Adv Anat Embryol Cell Biol*. 2012;212:1–115.
3. Slominski AT, Zmijewski MA, Zbytek B, Tobin DJ, Theoharides TC, Rivier J. Key role of CRF in the skin stress response system. *Endocr Rev*. 2013;34(6):827–884.
4. Nestle FO, Kaplan DH, Barker J. Mechanisms of disease: Psoriasis. *N Engl J Med*. 2009;361:496–509.
5. Singh TP, Zhang HH, Borek I, et al. Monocyte-derived inflammatory Langerhans cells and dermal dendritic cells mediate psoriasis-like inflammation. *Nat Commun*. 2016;7:13581.
6. Yoshiki R, Kabashima K, Honda T, et al. IL-23 from Langerhans cells is required for the development of imiquimod-induced psoriasis-like dermatitis by induction of IL-17A-producing γδ T cells. *J Invest Dermatol*. 2014;134(7):1912–1921.
7. Hartwig T, Pantelyushin S, Croxford AL, Kulig P, Becher B. Dermal IL-17-producing γδ T cells establish long-lived memory in the skin. *Eur J Immunol*. 2015;11:3022–3033.
8. Mason AR, Mason J, Cork M, Dooley G, Hancock H. Topical treatments for chronic plaque psoriasis. *Cochrane Database Syst Rev*. 2013;3:CD005028.
9. Prow TW, Grice JE, Lin LL, et al. Nanoparticles and microparticles for skin drug delivery. *Adv Drug Deliv Rev*. 2011;63(6):470–491.
10. Zhai Y, Zhai G. Advances in lipid-based colloid systems as drug carrier for topic delivery. *J Control Release*. 2014;193:90–99.
11. Lowes MA, Suárez-Fariñas M, Krueger JG. Immunology of psoriasis. *Annu Rev Immunol*. 2014;32:227–255.
12. Lin YK, Yang SH, Chen CC, Kao HC, Fang JY. Using imiquimod-induced psoriasis-like skin as a model to measure the skin penetration of anti-psoriatic drugs. *PLoS One*. 2015;10(9):e0137890.
13. van der Fits L, Mourits S, Voerman JS, et al. Imiquimod-induced psoriasis-like skin inflammation in mice is mediated via the IL-23/IL-17 axis. *J Immunol*. 2009;182(9):5836–5845.
14. Sun J, Zhao Y, Hu J. Curcumin inhibits imiquimod-induced psoriasis-like inflammation by inhibiting IL-1beta and IL-6 production in mice. *PLoS One*. 2013;8(6):e67078.
15. Meng F, Trivino A, Prasad D, Chauhan H. Investigation and correlation of drug polymer miscibility and molecular interactions by various approaches for the preparation of amorphous solid dispersions. *Eur J Pharm Sci*. 2015;71:12–24.
16. Zhao L, Fang L, Xu Y, Liu S, He Z, Zhao Y. Transdermal delivery of penetrants with differing lipophilicities using O-acylmenthol derivatives as penetration enhancers. *Eur J Pharm Biopharm*. 2008;69(1):199–213.
17. Mahler GJ, Esch MB, Tako E, et al. Oral exposure to polystyrene nanoparticles affects iron absorption. *Nat Nanotechnol*. 2012;7(4):264–271.
18. Vogt A, Combadiere B, Hadam S, et al. 40 nm, but not 750 or 1,500 nm, nanoparticles enter epidermal CD1a+ cells after transcutaneous application on human skin. *J Invest Dermatol*. 2006;126(6):1316–1322.
19. Wu JK, Siller G, Strutton G. Psoriasis induced by topical imiquimod. *Australas J Dermatol*. 2004;45(1):47–50.
20. Sun L, Cun D, Yuan B, et al. Formulation and in vitro/in vivo correlation of a drug-in-adhesive transdermal patch containing azasetron. *J Pharm Sci*. 2012;101(12):4540–4548.
21. Sun L, Liu Z, Wang L, et al. Enhanced topical penetration, system exposure and anti-psoriasis activity of two particle-sized, curcumin-loaded PLGA nanoparticles in hydrogel. *J Control Release*. 2017;254:44–54.
22. Wenkers BP, Lippold BC. Skin penetration of nonsteroidal antiinflammatory drugs out of a lipophilic vehicle: influence of the viable epidermis. *J Pharm Sci*. 1999;88(12):1326–1331.
23. Arimoto M, Fukumori Y, Fujiki J, Ichikawa H. Acrylic terpolymer microcapsules for colon-specific drug delivery: effect of molecular weight and solubility of microencapsulated drugs on their release behaviors. *J Drug Deliv Sci Technol*. 2006;16(3):173–181.
24. Kokate A, Li X, Williams PJ, Singh P, Jasti BR. In silico prediction of drug permeability across buccal mucosa. *Pharm Res*. 2009;26(5):1130–1139.
25. Brodin A, Nyqvist-Mayer A, Wadsten T, Forslund B, Broberg F. Phase diagram and aqueous solubility of the lidocaine-prilocaine binary system. *J Pharm Sci*. 1984;73(4):481–484.
26. Ho HO, Chen LC, Lin HM, Sheu MT. Penetration enhancement by menthol combined with a solubilization effect in a mixed solvent system. *J Control Release*. 1998;51(2–3):301–311.
27. Dias M, Hadgraft J, Lane ME. Influence of membrane-solvent-solute interactions on solute permeation in skin. *Int J Pharm*. 2007;340(1–2):65–70.
28. Garidel P, Fölting B, Schaller I, Kerth A. The microstructure of the stratum corneum lipid barrier: mid-infrared spectroscopic studies of hydrated ceramide:palmitic acid:cholesterol model systems. *Biophys Chem*. 2010;150(1–3):144–156.
29. Xie X, Tao Q, Zou Y, et al. PLGA nanoparticles improve the oral bioavailability of curcumin in rats: characterizations and mechanisms. *J Agric Food Chem*. 2011;59(17):9280–9289.
30. Lademann J, Knorr F, Richter H, et al. Hair follicles–an efficient storage and penetration pathway for topically applied substances. Summary of recent results obtained at the Center of Experimental and Applied Cutaneous Physiology, Charite -Universitatsmedizin Berlin, Germany. *Skin Pharmacol Physiol*. 2008;21(3):150–155.